Original Article

Molecular docking, ADMET, synthesis and anti-proliferative of novel derivatives of benzothiazine against lung cancer cell line

Haider Jabbar Al-Karagully[1*], Mohammed Kamil Hadi[2]

[1]Ministry of Health, The National Center of Drug Control and Research (NCDCR), Baghdad, Iraq. [2]Department of Pharmaceutical Chemistry, College of Pharmacy, University of Baghdad, Bagdad, Iraq.

Correspondence: Haider Jabbar Al-Karagully, Ministry of Health, The National Center of Drug Control and Research (NCDCR), Baghdad, Iraq. Haidar.Wasan2100p@copharm.uobaghdad.edu.iq

ABSTRACT

One of the most intriguing epigenetic targets for medication therapy is epidermal growth factor receptor tyrosine kinase (EGFR-TK). Overexpression of EGFR-TK is seen in many illnesses, including cancers. In the cnew EGFR-TK inhibitors were designed with the same consisting of erlotinib (approved anticancer drug) with longer linker and substituted hydrophobic moiety using Ligand Designer from Glide (Schrodinger LLC). By experimenting with different amide and Schiff base residues, the linker was optimized. Using licensed Schrodinger modeling software, the probable inhibition over EGFR-TK for the best-designed items was virtually assessed. The findings demonstrated that there is a possibility of an acceptable level of fitness interaction between the hydroxylated substitution hydrophobic moiety and the EGFR-TK active site. To forecast the final drugs' pharmacokinetic characteristics, an ADMET analysis was conducted. Good predicted drug-like characteristics were displayed by the final compounds. Recrystallization was used to successfully manufacture and purify the intermediates and final chemicals. FTIR, 1HNMR, and 13CNMR spectroscopy were used to characterize the chemical structure of the intermediates and final products. Using the MTT technique; all synthesized compounds (CN1-CN3) showed a reassuring antitumor performance in A504 lung cancer cells lines with IC50 of 7.58 μM, 10.08 μM, and 18.01 μM respectively, and inhibition percentages of 82.3%, 70.5%, and 65.2% respectively, which is comparable to erlotinib IC50 of 3.86 μM and inhibition percentage of 94.7%. The compound CN1 was the most promising one (IC50 = 7.58 μM and a percentage of inhibition=82.3%), compared with erlotinib, a reference authorized anticancer drug.

Keywords: ADMET, Anti-proliferative, Benzothiazine, Erlotinib, Lung cancer, Molecular docking

Introduction

Globally, there is a lot of focus on the discovery and development of anticancer medications. There are currently numerous substances in use, each with a unique antiproliferative mechanism of action. Alkylating agents, antimetabolites, cytotoxic antibiotics, alkaloids, plant medicines, and other categories are generally used to categorize antineoplastics. Complexing compounds from platinum cytostatic, protein kinase inhibitors, and monoclonal antibodies [1-4]. Compounds with potential efficacy that have higher pharmacodynamic and kinetic qualities and lower toxicity are still in high demand as therapeutic agents [5]. Different medications work well for different kinds of tumor growth. It can be said that one of the main issues that combination therapy attempts to solve is the resilience of tumor cells. Professionals and the general public are currently concentrating on the therapeutic application of nanoparticles and nano-formulated antineoplastics as well as a variety of drug-delivery nano-systems [6, 7]. Heterocycle combinations present a fresh chance to produce unique multicyclic molecules with enhanced biological activity [8]. Cell integrity and bodily balance depend on apoptosis, which is a type of controlled, self-automated cell death. Moreover, many illnesses, including breast cancer, can develop as a result of poor apoptotic process execution [9]. Therefore, one promising approach to treating hormone-

sensitive breast cancer is to target the regulators or inducers of apoptosis in cancer cells. The apoptogenic theory states that apoptotic signaling pathways can be induced and stimulated by aromatase inhibition, which suppresses estrogen production and lowers the risk of hormone-dependent breast cancer growth [10]. Heterocyclic compounds interact with a broad range of biological targets because of their structures [11-14], and they are crucial in the development of antineoplastics [15-19]. The primary feature of protease inhibitors that may be prescribed for their anti-tumor agent applications is their capacity to increase the susceptibility of cancer cells to chemotherapy and radiation [20]. In medicinal chemistry, the chief goal is to synthesize promising activity compounds acting as therapeutic agents with lower side effects [21]. A sulfur and nitrogen-containing scaffold, 1,4-benzothiazine (1,4-B), has attracted continuing interest and has become an important construction motif for developing new drug candidates [22]. The name 1,4-benzothiazine is applied to both 2H- and 4H-isomer of the molecule where 4H-1,4-benzothiazine analogs have been extensively studied for decades [23]. One of the most valuable structural features of 4H-1,4 benzothiazine to impart a diverse range of activity is the occurrence of the fold along the nitrogen and sulfur axis [24]. The compounds containing 4H-1,4 skeleton possess significant anticancer activity and many other biological activities such as central nervous system activity, anti-inflammatory, cardiovascular, and antimicrobial [25-29]. However, because of their widespread use and unique biological activity, Schiff bases have been extensively researched and are the subject of various studies [30]. One of the most common illnesses in the world is cancer. Lung cancer is one of the most prevalent malignancies and the primary cause of cancer-related mortality; in 2018 alone, it was responsible for about 1.7 million cancer-related deaths globally [31]. From a histological perspective, lung cancer can be classified into two types: small-cell lung cancer (SCLC) and non-small-cell lung cancer (NSCLC). About 85% of all lung cancers globally, including adenocarcinoma, squamous-cell carcinoma, and large-cell carcinoma, are caused by NSCLC [32, 33]. Even now, lung cancer is a fatal illness. Nonetheless, several advancements, including better diagnosis and the creation of novel medications, have resulted in a sharp increase in the five-year survival rate [34-37].

Materials and Methods

Molecular docking

A docking study was carried out using the Glide application, which is connected with the maestro software from the licensed Schrodinger's modeling suite version 13.0135. To create a novel Epidermal Growth Factor Receptor Tyrosine Kinase (EGFR_TK), Ligand Designer produced virtual molecules. The hydrophobic core, linker, terminal hydrophobic moiety, and terminal substitution of the proposed derivatives resembled the general pharmacophoric characteristics of erlotinib. With erlotinib as a co-crystallized ligand, the protein was selected from the homo sapiens to mimic a substance that would be effective on people. A protein data repository provides the EGFR-TK (4HJO) crystal structure [38]. The protein was preprocessed to assign bond order as part of the protein preparation wizard. Hydrogen was added, terminal oxygen was added to the chain, water beyond 3 A0 was removed from the ligand, water beyond 3 Ao from the ligand formed fewer than 3 hydrogen bonds with the ligand or amino acid had less chance of affecting the docking, from the active site, and het stat with EPiK was generated. The Schrodinger program 13.1 (1–2023) was used to optimize H-bond assignments with default settings and clean up the structure using the OPLS (2005) force field. Using the default configuration, which limited the grid size to 15A*15A*15A, the co-crystallized ligand that interacted with the protein was used to create the receptor grid. Using ligprep, which combines energy minimisation with the OPLS (2005) force field and takes into account tautomeric, stereochemical, and ionization states, the set of ligands to be docked is found and produced. This method goes beyond simple conversion of 2D and 3D structures. Using the default SP docking configuration, which limits out to 10 poses, the produced ligands were docked against EGFR (4HJO). The ligand's fitness in the active site was used to visualize the resulting poses.

ADMET studies

To evaluate the drug-likeness of the suggested compounds, the produced ligands are subjected to ligand-base ADMET prediction. The software was configured by QIKProp to find the five most similar drug molecules, and the output data was examined to determine the developed compounds' drug potential.

Chemical synthesis

Materials

The chemicals and solvents were purchased from different suppliers such as Sigma-Aldrich, Loba Chimei (India), hyper-chem (China), and Scharlau (Spain). Fine, were put to use without being further cleaned. Using a 20*20 cm TLC silica gel 60 F254 sheet from Merck KGaA, thin-layer chromatography (TLC) was carried out and detected at 254 nm UV light. The Shimadzu IRAffinity-1 Spectrometer (Shimadzu, Japan) was used to perform FT IR spectroscopy at the University of Baghdad's College of Pharmacy's Pharmaceutical Chemistry department. The Mansoura University-Faculty of Pharmacy conducted 1HNMR analyses at 400 MHz and 13C-NMR at 100 MHz (with d6-DMSO as the solvent) using a Bruker Avance III.

General procedure for the synthesis of ethyl 4H-benzo[b][1,4]thiazine-3-carboxylate (compound A) [39]

A mixture of ethyl bromopyruvate (0.01 mol) and 2-amino-5-substituted thiophenol (0.01 mol) in 50 ml of absolute ethanol was stirred continuously in RBF for 18 hours before being allowed to cool. The precipitate was filtered through ash-free filter paper, cleaned, and purified by recrystallization from ethyl alcohol, yielding a yellow powder that was 78% pure. I.R: 3047, 2978, 2935, 2900, 1708, 1608, 1577, 1442, 1226, 1087 and 780 cm^{-1}. ^{1}HNMR (400 MHz, DMSO) δ 7.71 – 7.62 (m, 1H, Ar-CH), 7.49– 7.34 (m, 3H, Ar-CH), 4.24 – 4.12 (m, 2H, CH2), 1.22 (t, 3H, CH3). ^{13}CNMR: δ 161, 149, 133, 131, 128, 126, 123, 117, 115, 62.66 and 13.98

General procedure for synthesis of 4H-benzo[b][1,4]thiazine-3-carbohydrazide (compound B) [40]

A solution of 0.01 mol of (compound A) in 30 mL of absolute methanol, hydrazine hydrate (0.1 mol, 80%) was added step by step in a 100 ml RBF, followed by a catalytic amount of conc. H2SO4 (10 drops). The reaction mixture was refluxed for 8 h. The solid powder separated and excess solvent was removed. The residue was recrystallized from methanol and the product dried to yield (82%) an orange crystalline powder. I.R: 3387, 3340, 3286, 3248, 3197, 3159, 2904, 1670, 1612, 1581, 1500, 1473, 1396, 1053 and 741 cm^{-1}. ^{1}HNMR (400 MHz, DMSO) δ 9.35 (s, 1H, Acyc-NH), 7.59 (s, 1H, Ar-CH), 7.03 – 6.95 (m, 1H, Ar-CH), 6.91 – 6.84 (m, 2H, Ar-CH), 6.74 (s, 1H, Cyc-NH), 4.38 (d, J = 3.9 Hz, 2H, NH2). ^{13}CNMR: δ 167, 156, 131, 129, 128, 126, 123, 118 and 115.

General procedure for the synthesis of hydrazide derivatives (CN1–CN3) [41]

A mixture of the hydrazide (compound B) (0.01mol) and para-substituted phenyl isocyanate (0.02 mol) in dry benzene (80 ml) was refluxed for 14 hr in a steam bath. TLC monitored the reaction until the precipitate appeared. The precipitate was collected by evaporating the excess solvent and then filtration using an ash-free filter paper. It was recrystallized by methanol to give a finished product (CN1-CN3).

Compound **CN1** yield is (77%) as an orange-colored powder; I.R: 3363, 3340, 3298, 3194, 3093, 2931, 2904, 1720, 1685, 1639, 1600, 1543, 1469, 1361, 1095 and 732 cm^{-1}. ^{1}HNMR (400 MHz, DMSO) δ10.29 (s, 1H, Acyc-NH), 8.57 (s, 2H, Acyc-NH), 7.58 – 7.53 (m, 1H, Ar-CH), 7.52 – 7.47 (m, 1H), 7.40 – 7.31 (m, 1H, Ar-CH), 7.34 – 7.27 (m, 1H, Ar CH), 7.11 – 7.02 (m, 2H, arCH), 6.86 (s, 1H, Cyc-NH), 6.72 – 6.64 (m, 2H, Ar CH).^{13}CNMR: δ 168.7, 160, 155, 142,141, 138, 129, 128.99, 128.9, 128.8, 123, 120.8, 120.5, 120.3, and 118.

Compound **CN2** yield is (72%) as a gray-colored powder; I.R: 3309, 3016, 2970, 2943, 1739,1685, 1651, 1620, 1577, 1465, 1365, 1226, 1215, 1153,1160, 929 and 744 cm^{-1}. ^{1}HNMR (400 MHz, DMSO) δ 10.38 (s, 1H, Acyc-NH), 9.69 (s, 1H, Acyc-NH), 8.48(s, 1H, Acycl-NH), 8.24 (s, 1H, Acycl-NH), 7.76-773 (m, 2H, Ar-CH), 7.58 – 753 (m, 2H, Ar CH), 7.07 – 7.03 (m, 2H, Acyc-NHH), 6.87 (s, 1H, Cyc-NH). ^{13}CNMR: δ 168.7, 160, 152, 142, 141, 128.8, 128.5, 127.9, 127.1, 126.6, 125.6, 125.4, 123 and 118.

Compound **CN3** yield is (76%) as a pale-brawn colored powder; I.R: 3340, 3302, 3224, 3105, 2908, 1720, 1689, 1651, 1620, 1554, 1482, 1477, 1415, 1327, 1300, 1246, 1176, 1111, 1037, 848 and 748 cm^{-1}. ^{1}HNMR (400 MHz, DMSO) δ 9.94(s, 1H, Acyc-NH), 9.11(s, 1H, Acyc-NH), 8.36(s, 1H, Acyc-NH), 7.54 – 7.48 (m, 2H, Ar CH), 7.44 – 7.35 (m, 1H, Ar-CH), 7.24- 715 (m, 2H, Ar CH), 7.11 – 7.01 (m, 3H, Ar-CH), 6.93 (s, 1H, Cyc-NH). ^{13}CNMR: δ 166, 160, 152, 140, 139, 132.6,132., 129, 127, 126, 124, 121 and 120.

Antiproliferative activity evaluation [42]

For academic purposes, the human cancer cell line A504 (small cell lung carcinoma) was obtained. Normal lung cells (NL-20) were cultured in moist conditions at 37°C with 5% CO2 and 95% air. Fresh medium was administered every two days and 24 hours before the experiments' conclusion. Pre-confluent bulks of cells were passaged using a solution containing 0.05% trypsin and 0.5 mM EDTA. The Biotechnology Research Centre at Al-Nahrain University maintained and examined cell lines that were kept in liquid nitrogen. The antiproliferative effectiveness of the final compounds was measured in vitro using the MTT test. Cells that were exponentially budding were created and plated in 96-well plates at a density of 1x104 cells/well. The cells in the wells were incubated for 24 hours at 37°C with humidified 5% CO2 to allow for cell accessory, and then they were treated for 48 hours with chemicals (CN1-CN3) at progressively higher concentrations. The cells were not harmed by the DMSO concentration, which was consistently maintained far below 1.25%. Phosphate-buffered saline (PBS; 1.5 mM KH2PO4, 6.5 mM Na2HPO4, 137 mM NaCl, 2.7 mM KCl; pH 7.4) was used to dissolve 3-(4,5-dimethylthizao1–2-y1)-2,5-diphenyltetrazolium bromide (MTT) at a concentration of 5 mg/mL. Each well received 20 µL of this solution added to it. The medium/MTT mixes were separated and the formazan crystals produced by the mitochondrial dehydrogenase activity of energetic cells were dissolved in 100 µL of DMSO per well after the cells were cultivated for four hours at 37°C in a dampened incubator with 5% CO2. The absorbance of the wells at 570 nm was measured using a Bio-Rad Instruments microplate reader. Cells that had been preserved using DMSO as a control in the ELASIS device were used to calculate the chemical's effects on cell viability, and the optical density measurements were statistically analysed to estimate the IC50.

Results and Discussion

Erlotinib had a docking score of -9.458 kcal/mol in the Docking Study, while the suggested derivatives of CN1, CN2, and CN3 had docking scores of -6.536, -5.848, and -6.772 kcal/mol, respectively. By populating the active site with the majority of

interactions of active site protein amino acids, the proposed compounds demonstrated an acceptable active site fitness **(Figure 1)**.
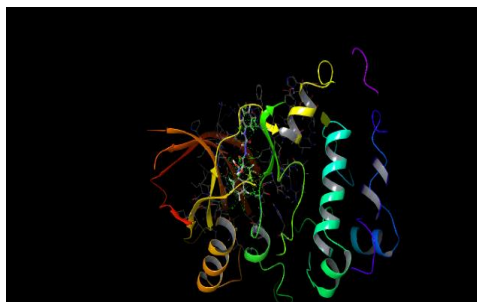

Figure 1. The 3D poses for the interaction of compound CN1 with EGFR-TK isoform (4JHO)

Redocking the co-crystallized ligand into the corresponding receptor's active center and determining the root mean square deviation (RMSD) for the suggested docking algorithm's repeatability and dependability was the first step in validating the molecular modeling technique. The RMSD 0.56 Å was smaller than 2.00 Å when the co-crystallized ligand was docked independently on EGFR-tyrosine kinase (4HJO), indicating that the algorithm was validated in comparison to the crystallographic structure. All derivatives provide an approved receptor fitness by forming a connection with many residues inside the active site, according to a close visual examination of the 2D ligand-receptor interaction. According to the docking results, all of the docked derivatives (CN1–CN3) have binding energies in the protein's active site that are similar to erlotinib's, indicating a possible interaction with the EGFR protein, which binds via hydrogen bonding in addition to other brief contacts that enhance binding. The docking results for all synthesized derivatives (CN1-CN3) revealed a water bridge Hydrogen bond with THR830, and THR766 via carbonyl moiety; as well derivative (CN2) formed two other hydrogen bonds one with MET769 via NH- amide moiety, and the other with LYS704 via oxygens of terminal NO2 moiety; additionally, all synthesized derivatives form 3 hydrophobic interactions with (ALA919, LEU764, and PRO770), 1 polar interaction with THR830, and one charged interaction with LYS721. The erlotinib revealed two hydrogen bonds with MET769 and CYS773 and one water bridge hydrogen bond with THR830, and THR766; in addition to the 9 short connects listed above **(Figure 2)**.
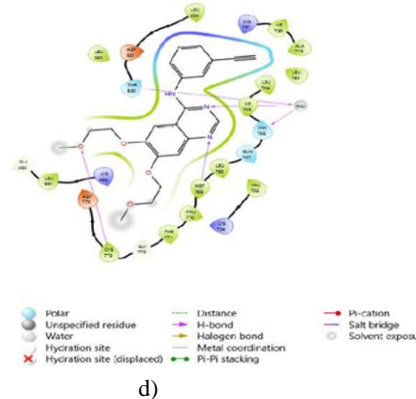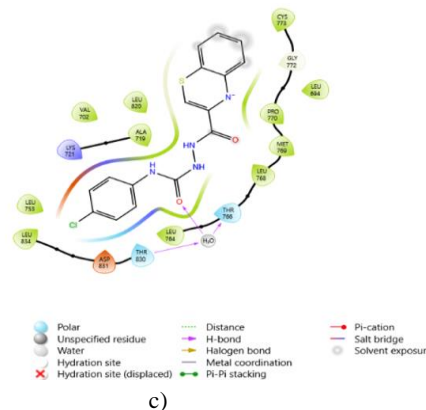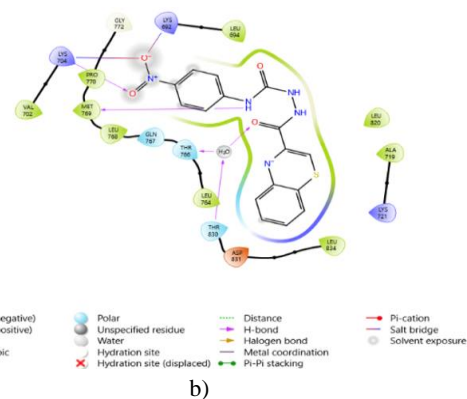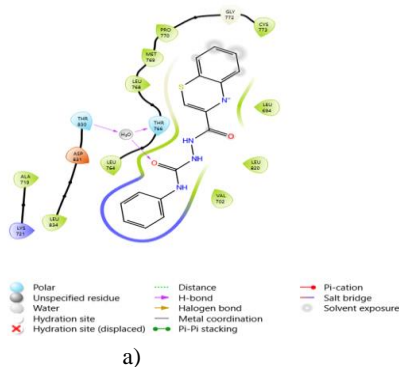

Figure 2. Two-Dimensional Interaction Diagram of (a) CN1, (b) CN2, (c) CN3, and (d) Erlotinib with EGFR-TK (4HJO).

ADME-TOX studies

For the designed molecules to be regarded as drug-like molecules, a number of structural characteristics and attributes must be taken into account. For example, the rule of three and the rule of five for drugs taken orally are essential strategies for preventing costly late preclinical trials and clinical trial frustration. Acceptable estimated pharmacokinetic parameters were displayed by all synthesized compounds (CN1–CN3). The findings showed a tendency for hydrogen bonding as well as metabolic stability. Furthermore, the compounds do not violate the principles governing drug-like molecules and have a respectable calculated oral absorptivity **(Table 1)**.

Compound	CNS	#metab	Human Oral Absorption	Rule of five	Rule of three
CN1	-1	4	3	0	0
CN2	-2	4	2	0	0
CN3	-1	3	3	0	0
Erlotinib	-1	6	3	0	1

Chemical synthesis

As shown, **Figure 3** demonstrates the synthesis steps of intermediate compounds A & B. The synthesis involves ester formation starting from p-amino benzenethiol reaction with ethyl 3-bromo-2-oxopropanoate to afford benzothiazine ring with acyclic ester (compound A), which is converted to an amid-containing compound (hydrazide of benzothiazine). Then, new carbohydrazides were prepared by condensing the lately synthesized compound (B) with different cyclic aldehydes giving final compounds (CN1, CN2, and CN3), respectively .
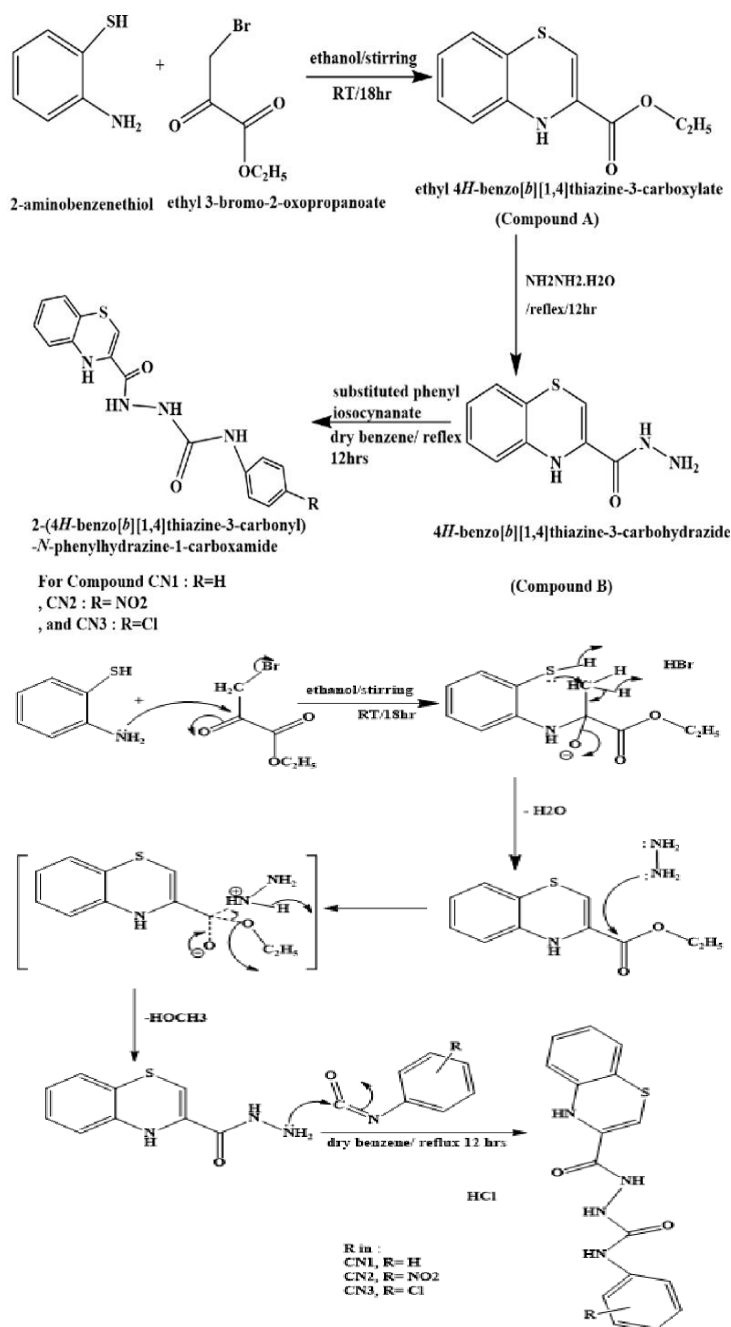

Figure 3. Synthetic pathway of new derivatives CN1-CN3

Compound studies using thin-layer chromatography were carried out on aluminum foils coated with silica gel. On the aluminum foils, the compound solutions were placed at a spot approximately 2 cm above the lower edge. The polarity of the

chemicals determined the chosen mobile phases (Ethyl acetate: hexane). Equipment for measuring the open capillary melting point was used to determine the melting points of synthetic substances. Chemical shifts were expressed in parts per million (δ), and signals were classified as multiple (m), singlet (s), doublet (d), and triplet (t). Compounds were analyzed using thin-layer chromatography, with the polarity of the compounds dictating the preferred mobile phases (ethyl acetate: hexane). The synthesized compounds were characterized, and their structures were verified by "FTIR, ¹HNMR & ¹³CNMR" spectral analyses.

IR spectra for compounds (A) show characteristic band 1708 ester(C=O), 1674 (C=N), and disappearance of band 1732 (C=O of the acyclic ester of ethyl 3-bromo-2-oxopropanoate). However, compound B shows the disappearance of the ester band and formation of the amide band at (1670) and the appearance of additional bands of NH and NH2 of hydrazide (3387, 3340 &3244 (NH & NH2). Also, additional bands at attributed to (Ar-CH stretching) of additional aryl ring and the disappearance of a band of NH2 of hydrazide in all final compounds (CN1-CN3) with little differentiation among them such as the appearance of two amid (C=O) bands which were 1720, 1685for CN1, 1739,1685 for CN2, and 1720, 1689 for CN3.

¹HNMR spectra of the compounds were agreeable with the assigned structures; Compounds (A) show signals at δ= 4.24 – 4.12 (m, 2H, CH2), 1.22 (t, 3H, CH3) ppm they will disappear in case of hydrazide compound (B) and instead appeared of 9.35 (s, 1H, Acyc-NH) and 4.38 (s, 2H, NH2); for CN1 clear additional signals for additional aryl ring and disappearance of the signal of 4.38 (d, 2H, NH2 of compound B); instead appearance of new NH signals of acyclic amides formed in final compounds, for CN1 appearance of 10.29 (s, 1H, Acyc-NH), 8.57 (s, 2H, Acyc-NH), for CN2 appearance of 10.38 (s, 1H, Acyc-NH), 9.69 (s, 1H, Acyc-NH), 8.48(s, 1H, Acycl-NH) and for CN3 appearance of 9.94(s, 1H, Acyc-NH), 9.11(s, 1H, Acyc-NH), 8.36(s, 1H, Acyc-NH).

¹³C NMR spectra of the compounds were agreeable with the assigned structures; Compound A has specific signals at 161.36 for ester carbonyl carbon, 62.66 for CH2, and 13.98 for CH3; these signals will disappear in hydrazide instead of the appearance of signals at 167.45 for amide carbon; in final compounds (CN1-CN3) appear of signals of new carbons of new amide formed, which were 168.7, 160, 155 for CN1, 168.7, 160, 152 for CN2, and 166, 160, 152 for CN3

Anti-proliferative analysis

Survival (%) = [(absorbance of treated cells-absorbance of culture media)/(absorbance of untreated cells-absorbance of culture medium)] x 100 was the formula used to determine cell persistence. The inhibitory concentration (IC) values were determined using a dose-response curve in a triplicate experiment. The concentration in "µM" needed to inhibit cell growth by 50% when compared to a control is known as the "IC50." monoclonal (Erlotinib) as a reference. From the

rectilinear section of the curve, IC50 values were obtained by determining the agent's concentration that reduced absorbance in pickled cells by 50% when compared to control cells. The estimate is derived from three independent experiments with a minimum of six microcultures per concentration level. As will noted in **Figures 1, 2 and 4**, and **Table 2** the inhibition % and inhibitory concentration (IC50) of all synthesized compounds (CN1-CN3) showed good results of inhibition% 82.3%, 70.5%, and 65.2%; and IC50 7.58 µM, 10.08 µM, and 18.01 µM for finished products (CN1-CN3) respectively; compared with the inhibition % (94.7%) and IC50 (3.86µM) for reference approved drug (erlotinib); the most promise derivative was CN1 possess inhibition% (82.3%) and IC50 (7.58µM, that's maybe corresponding to SAR of these derivatives and the tyrosine kinase receptor were they must act as anti-proliferative against lung cancer cell line.

Structure-activity relationships (SAR)

Useful information regarding the structure-activity relationships (SAR) of the newly synthesized derivatives of 2-(4H-benzo[b][1,4]thiazine-3-carbonyl)-N-phenylhydrazine-1-carboxamide (CN1-CN3), as potential EGFR-TK inhibitors, can be highlighted by comparing their structure to erlotinib, specifically those moieties on the reference compounds that make them successful cytotoxic medications. All synthesized derivatives are composed of the same structural skeletons of the hydrophobic center (benzothiazine ring), linker (two amide groups), terminal hydrophobic moiety (benzene ring), and terminal substitution except in CN1; the difference in the activity of synthesized derivatives may be due to the difference in their fitting in receptor pocket; the presence of unsubstituted benzene ring give the most anti-proliferative activity (i.e. lower IC50 value) (compound CN1), then *p*- nitro benzene ring (compound CN2), then *p*-chloro substituted compound CN3. All the synthesized compounds have IC50 less than 20 µM, which indicates a good structural skeleton to give good anti-proliferative activity against small cell lung cancer cell lines [43-45].
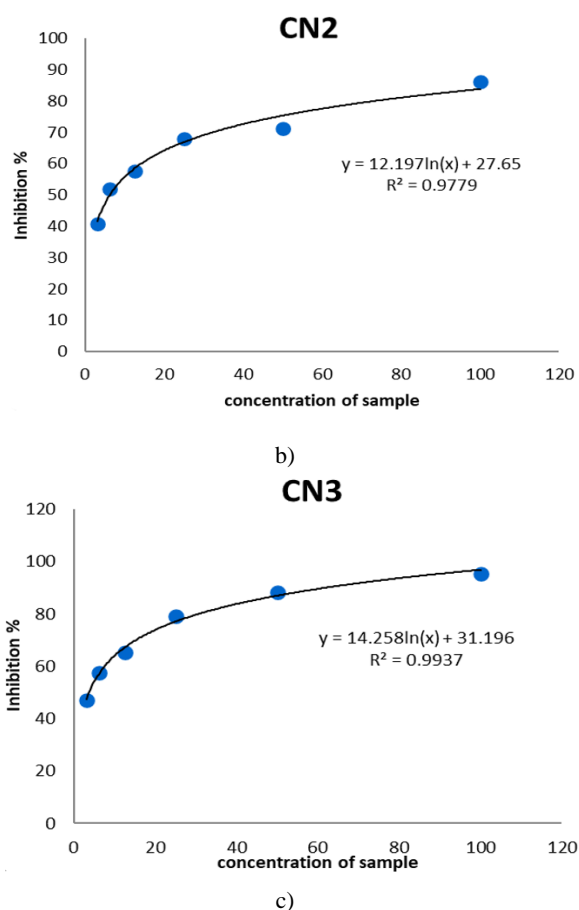

a)
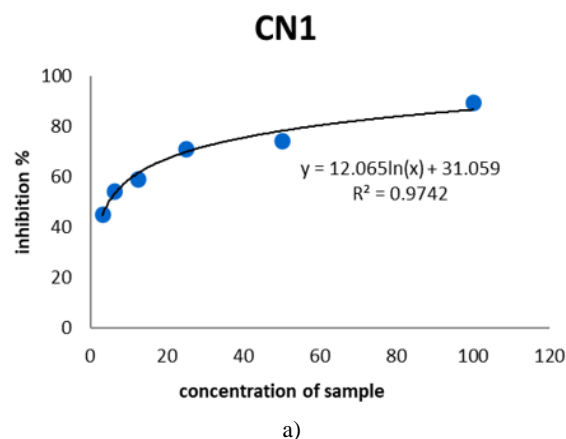
Figure 4. Dose-response curve of (a): CN1, (b): CN2, (c): CN3.

Table 2. Inhibition% and IC50 of Erlotinib and synthetic derivatives CN1-CN3

	Inhibition %	IC50(μM)
CN1	82.3	7.58
CN2	70.5	10.08
CN3	65.2	18.01
Erlotinib	94.7	3.86

Conclusion

Possibility By adding novel compounds with double amide groups, EGFR-TK inhibitors were created. The licensed Glide program was used to conduct molecular docking investigations on the freshly produced molecules. Although the final compounds had a lower docking score and were practically attached to EGFR-TK, they are still linked to protein amino acids by a variety of interactions, including hydrogen bonds, which have a recognized level of fitness. The virtual ADMET experiments revealed that the final drugs had acceptable pharmacokinetic characteristics. Excellent mild organic synthesis techniques were used to effectively synthesize the specified compounds with acceptable yields. FTIR, 1HNMR, and 13CNMR spectroscopy were used to characterize each of the intermediates and end products. According to the antiproliferative activity investigation, the synthesized compounds showed a promising preliminary inhibition of cancer cells that is similar to that of erlotinib, a tyrosine kinase inhibitor that is employed in clinical settings. With an inhibition percentage of 82.3% and the lowest IC50 (7.58μM), compound CN1 demonstrated the highest cytotoxicity against the A-504 lung cancer cell line.

References

1. Jampilek J, Kralova K. Insights into lipid-based delivery nanosystems of protein-tyrosine kinase inhibitors for cancer therapy. Pharmaceutics. 2022;14(12):2706.

2. Pottier C, Fresnais M, Gilon M, Jérusalem G, Longuespée R, Sounni NE. Tyrosine kinase inhibitors in cancer: Breakthrough and challenges of targeted therapy. Cancers (Basel). 2020;12(3):731.

3. Zahavi D, Weiner L. Monoclonal antibodies in cancer therapy. Antibodies (Basel). 2020;9(3):34.

4. Jin S, Sun Y, Liang X, Gu X, Ning J, Xu Y, et al. Emerging new therapeutic antibody derivatives for cancer treatment. Signal Transduct Target Ther. 2022;7(1):39.

5. Hadi MK, Rahim NA, Sulaiman AT, Ali RM. Synthesis, characterization and preliminary antimicrobial evaluation of new schiff bases and aminothiadiazole derivatives of N-substituted phthalimide. Res J Pharm Technol. 2022;15(9):3861-5.

6. Jampilek J, Kralova K. Anticancer applications of essential oils formulated into lipid-based delivery nanosystems. Pharmaceutics. 2022;14(12):2681.

7. Yang T, Zhai J, Hu D, Yang R, Wang G, Li Y, et al. "Targeting design" of nanoparticles in tumor therapy. Pharmaceutics. 2022;14(9):1919.

8. Abdulraheem SS, Hadi MK. Synthesis and characterization of new coumarin derivatives as possible antimicrobial agents. Int J Drug Deliv Technol. 2021;11(4):1484-90.

9. Fayed EA, Eissa SI, Bayoumi AH, Gohar NA, Mehany ABM, Ammar YA. Design, synthesis, cytotoxicity and molecular modeling studies of some novel fluorinated pyrazole-based heterocycles as anticancer and apoptosis-inducing agents. Mol Divers. 2019;23(1):165-81.

10. Vinsova J, Cermakova K, Tomeckova A, Ceckova M, Jampilek J, Cermak P, et al. Synthesis and antimicrobial evaluation of new 2-substituted 5,7-di-tert-butylbenzoxazoles. Bioorg Med Chem. 2006;14(17):5850-65.

11. Fajkusova D, Pesko M, Keltosova S, Guo J, Oktabec Z, Vejsova M, et al. Anti-infective and herbicidal activity of N-substituted 2-aminobenzothiazoles. Bioorg Med Chem. 2012;20(24):7059-68.

12. Imramovský A, Pejchal V, Štěpánková Š, Vorčáková K, Jampílek J, Vančo J, et al. Synthesis and in vitro evaluation of new derivatives of 2-substituted-6-fluorobenzo [d] thiazoles as cholinesterase inhibitors. Bioorg Med Chem. 2013;21(7):1735-48.

13. Taylor AP, Robinson RP, Fobian YM, Blakemore DC, Jones LH, Fadeyi O. Modern advances in heterocyclic chemistry in drug discovery. Org Biomol Chem. 2016;14(28):6611-37.

14. Pearce S. The importance of heterocyclic compounds in anti-cancer drug design. Drug Discovery World. 2017;18(2):66-70. Available from: https://www.ddw-online.com/the-importance-of-heterocyclic-compounds-in-anti-cancer-drug-design-1106-201708/ (accessed on 10 February 2023).

15. Ali I, Lone MN, Al-Othman ZA, Al-Warthan A, Sanagi MM. Heterocyclic scaffolds: Centrality in anticancer drug development. Curr Drug Targets. 2015;16(7):711-34.

16. Lang DK, Kaur R, Arora R, Saini B, Arora S. Nitrogen-containing heterocycles as anticancer agents: An overview. Anticancer Agents Med Chem. 2020;20(18):2150-68.

17. Amewu RK, Sakyi PO, Osei-Safo D, Addae-Mensah I. Synthetic and naturally occurring heterocyclic anticancer compounds with multiple biological targets. Molecules. 2021;26(23):7134.

18. Martins P, Jesus J, Santos S, Raposo LR, Roma-Rodrigues C, Baptista PV, et al. Heterocyclic anticancer compounds: Recent advances and the paradigm shift towards the use of nanomedicine's tool box. Molecules. 2015;20(9):16852-91.

19. Banik BK, Banerjee B. Heterocyclic anticancer agents. De Gruyter: Berlin, Germany; 2022.

20. Hmood KS, Kubba AARM. Synthesis, docking study and in vitro anticancer evaluation of new derivatives of 2-(1-(2-Flouro-[1,1- Biphenyl]-4-Yl)Ethyl)-6-(Substituted Phenyl) imidazole[2,1-B][1,3,4]thiadiazole derived from flurbiprofen. Sys Rev Pharm. 2021;12(2):184.

21. Sahib HA, Hadi MK, Abdulkadir MQ. Synthesis, and antimicrobial evaluation of new hydrazone derivatives of (2, 4-dinitrophenyl) hydrazine. Res J Pharm Technol. 2022;15(4):1743-8.

22. Pratap UR, Jawale DV, Londhe BS, Mane RA. Baker's yeast catalyzed synthesis of 1, 4-benzothiazines, performed under ultrasonication. J Mol Catal B Enzym. 2011;68(1):94-7.

23. Gupta RR, Jain M, Rathore RS, Gupta A. Synthetic and spectral investigation of fluorinated phenothiazines and 4H-1, 4-benzothiazines as potent anticancer agents. J Fluor Chem. 1993;62(2-3):191-200.

24. King DJ, Wager E. Haematological safety of antipsychotic drugs. J Psychopharmacol. 1998;12(3):283-8.

25. Cecchetti V, Calderone V, Tabarrini O, Sabatini S, Filipponi E, Testai L, et al. Highly potent 1,4-benzothiazine derivatives as K(ATP)-channel openers. J Med Chem. 2003;46(17):3670-9.

26. Deshmukh MB, Mulik AR, Dhongade-Desai S. Synthesis of some new 2-Methyl-1, 4-benzothiazine-3 (1H)-one derivatives as potential vasodilators. J Chem. 2004;1(4):206-10.

27. Kajino M, Mizuno K, Tawada H, Shibouta Y, Nishikawa K, Meguro K. Synthesis and biological activities of new 1, 4-benzothiazine derivatives. Chem Pharm Bull. 1991;39(11):2888-95.

28. Rathore BS, Kumar M. Synthesis of 7-chloro-5-trifluoromethyl/7-fluoro/7-trifluoromethyl-4H-1,4-benzothiazines as antimicrobial agents. Bioorg Med Chem. 2006;14(16):5678-82.

29. Macchiarulo A, Costantino G, Fringuelli D, Vecchiarelli A, Schiaffella F, Fringuelli R. 1,4-Benzothiazine and 1,4-benzoxazine imidazole derivatives with antifungal activity: A docking study. Bioorg Med Chem. 2002;10(11):3415-23.

30. Ahmed WS, Mahmood AA, Al-Bayati RI. Synthesis and evaluation of antimicrobial activity of new imides and schiff bases derived from Ethyl-4-Amino Benzoate. Oriental J Chem. 2018;34(5):2478.

31. Bray F, Ferlay J, Soerjomataram I, Siegel RL, Torre LA, Jemal A. Global cancer statistics 2018: Globocan estimates of incidence and mortality worldwide for 36 cancers in 185 countries. CA Cancer J Clin. 2018;68(6):394-424.

32. Inamura K. Lung cancer: Understanding its molecular pathology and the 2015 WHO classification. Front Oncol. 2017;7:193.

33. Han Y, Li H. miRNAs as biomarkers and for the early detection of non-small cell lung cancer (NSCLC). J Thorac Dis. 2018;10(5):3119-31.

34. Scagliotti G, Stahel RA, Rosell R, Thatcher N, Soria JC. ALK translocation and crizotinib in non-small cell lung cancer: An evolving paradigm in oncology drug development. Eur J Cancer. 2012;48(7):961-73.

35. Sequist LV, Bell DW, Lynch TJ, Haber DA. Molecular predictors of response to epidermal growth factor receptor antagonists in non-small-cell lung cancer. J Clin Oncol. 2007;25(5):587-95.

36. Woodman C, Vundu G, George A, Wilson CM. Applications and strategies in nanodiagnosis and nanotherapy in lung cancer. Semin Cancer Biol. 2021;69:349-64.

37. Park JH, Liu Y, Lemmon MA, Radhakrishnan R. Erlotinib binds both inactive and active conformations of the EGFR tyrosine kinase domain. Biochem J. 2012;448(3):417-23.

38. Kisszékelyi P, Peňaška T, Stankovianska K, Mečiarová M, Šebesta R. Derivatives of benzo-1,4-thiazine-3-carboxylic acid and the corresponding amino acid conjugates. Beilstein J Org Chem. 2022;18:1195-202.

39. Kamms ZD, Hadi MK. Synthesis, characterization and preliminary antimicrobial and anti-inflammatory evaluation of new ibuprofen hydrazide derivatives. Int J Drug Deliv Technol. 2023;13(1):376-38.

40. Abduljabbar TT, Hadi MK. Synthesis, characterization and antibacterial evaluation of some coumarin derivatives. Iraqi J Pharm Sci. 2021;30(1):252.

41. Mohamed FK. Synthesis, reactions and antimicrobial activity on some novel phthalazinone derivatives. Egypt J Chem. 2010;53(5):645-60.

42. Hassan OM, Razzak Mahmood AA, Hamzah AH, Tahtamouni LH. Design, synthesis, and molecular docking studies of 5- bromoindole-2-carboxylic acid hydrazone derivatives: In vitro anticancer and VEGFR-2 inhibitory effects. Chemistry Select. 2022;7(9):3726.

43. Avramova N, Vasileva IM. The effects of continuing postgraduate education and career breaks on satisfaction levels among dentists in Bulgaria. Ann Dent Spec. 2023;11(2):106.

44. Ansari SH, Ahmed S, Abdulaziz LN, AlRumayyan SM, Mostafa MA, Al-Mohammed RS, et al. Wound healing of cyanoacrylate vs collagen among patients undergoing oral surgery: A systematic review. Ann Dent Spec. 2023;11(4):56-61.

45. Mishununa VV, Chapanov MM, Gakaeva KI, Tsoroeva MB, Kazanova SA, Gorlova MI, et al. Computed quantum chemical modeling of the effect of nanosilver on coronavirus COVID-19. Pharmacophore. 2021;12(2-2021):14-21.